Digitizations and Occupancies for Tracking in LHCB

Marcel Merk[1]
University of Utrecht

Abstract

A flexible framework to test the performance of various detector techniques for tracking in LHCB has been developed and implemented in the SICB simulation program. In this framework, a detector response to traversing particles in $B\bar{B}$ events is simulated. The calculations include a parametrization for efficiency and resolution for each channel. The chamber segmentation and granulation is governed by limits on drift time and hit multiplicities. The occupancy numbers for a final layout of stations are presented.

1 Introduction

This note describes the simulated detector response of the tracking stations in the framework of the LHCB simulation program SICB [1]. The tracking stations consist of an inner part of high granularity detectors and an outer part with moderate granularities.

In the detector response program we have emphasized flexibility. Different technologies can be tested in the same framework, with a simple change of a few parameters. In this note the software framework is discussed, not the individual detector technologies.

The outer tracker detectors consists of drift chamber modules characterized by their geometric acceptance, cell efficiency and measurement resolution. The exact shape of the cell, whether hexagonal, round or elliptical is only of secondary importance.

In the inner tracker we can accomodate different technologies as MSGC, MCSC or silicon, by chosing different response parameters.

The flexibility is also kept for the overal layout of a station. The number of single layers (or monolayers) inside each station is a free parameter, as is the stereo angle of each of the monolayers.

The price of this flexibility is a limited level of detail in the GEANT simulation. In the GEANT tracking step a station is simply represented as a homogeneous slice of material with a given thickness. Only the entrance and

[1]The research of M. Merk has been made possible by a fellowship of the Royal Netherlands Academy of Arts and Sciences

exit points of a track traversing the station are recorded as is the total energy loss. The specific detector response is taken into account in what is called the digitization process, which is done together with the track reconstruction.

2 Digitizations

The digitizations provide the detector response to a traversing track. From the stored track entrance and exit point in a generic measurement station the specific detector responses are derived.

Outer Tracker Digitizations

The outer tracker provides a measurement of the drift time of a traversing particle to the anode wire (fig 1a). We assume that the cell is triggered by electrons originating from the closest point of the track to the wire. We assume the drift r-t relation to be perfectly known. In this case we don't explicitly generate drift times, but convolute the the drift distance with a Gaussian resolution function σ, which is parameterized as a function of the position in the cell (fig 1b).

The parametrization used to simulate the resolution is:

$$\sigma = p_1 + p_2 \cdot e^{-\frac{r^2}{2p_3^2}}$$

The parameters p_1, p_2 and p_3 are taken from measurements and detailed MC calculations for candidate gas mixtures for LHCB [3]. Their values depend on the strength of the magnetic field present in the chambers. Typical parameter settings with and without B field are given in table 1.

	Outer Tracker		Inner Tracker	
	B=0 T	B=1 T	B=0 T	B=1 T
p_1	80 μm	110 μm	70 μm	70 μm
p_2	130 μm	180 μm	0	0
p_3	1.40 mm	1.40 mm	0	0

Table 1: Typical resolution parameters used in the simulations. p_1 is the resolution far away from the anode wire, $p_1 + p_2$ is the resolution at the wire. Parameter p_3 defines the scale of "far away" and "close to" the anode wire.

The geometry of two staggered layers of drift cells is shown in fig 2, in this case for a honeycomb cell. This layout gives a geometrical acceptance of

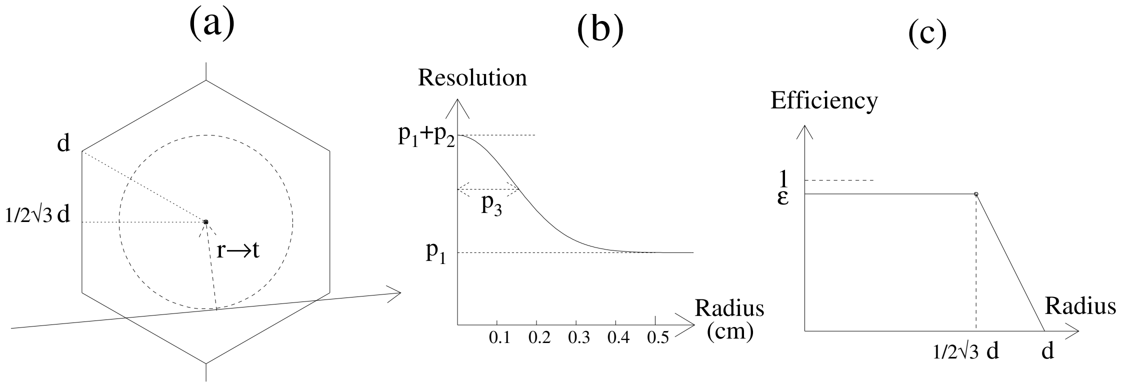

Figure 1: (a) A track traversing a drift chamber cell with minimal distance r. The maximum distance in a cell is d, the closest distance of a wall to the wire is $\frac{1}{2}\sqrt{3}d$. (b) The resolution as function of the position in the cell in terms of the resolution parameters p_1, p_2, p_3. (c) The parametrized cell efficiency as a function of the drift distance r.

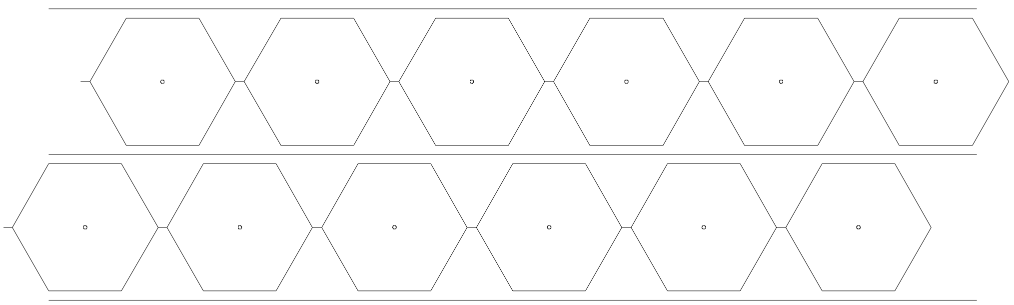

Figure 2: Schematic view of a honeycomb double layer. The geometrical acceptance of the staggered double layer is approximately 100%.

89% per single layer for cell size of 8 mm and 82% for cell size of 5 mm. The geometric acceptance for a staggered double layer is almost 100%.

In addition to the geometrical acceptance a cell efficiency is included. The cell efficiency is plotted in fig 1. This efficiency takes into account a reduced efficiency if a track passes near the edge of a hexagonal cell. Elsewhere we have assumed an efficiency of $\varepsilon = 98\%$.

Inner Tracker Digitizations

The inner tracker detectors measure a track impact point in a plane perpendicular to the beam axis. The measured linear coordinate is perpendicular to the strip orientation and is assumed to be measured with a Gaussian resolution σ. The resolution is taken to be position independent and can be chosen to match the expected resolution of the technology under study. Here we have used 70 μm.

The inner tracker is assumed to have have a 100% geometrical acceptance.

3 Station Segmentation

In the simulation program the tracking stations are segmented as shown in fig 3. The actual size of each of the sectors in a layer is defined by the parameters x_i and y_i. In the inner tracker the setup allows for implementation of two different technologies with smaller (sector I and II) and larger (sector III and IV) pitch sizes. In the outer tracker chambers of type I and II have smaller cell size than those of type III. The segmentation is driven by requirements of occupancy and drift time. The sectioning is chosen such that occupancies are lower than 10% everywhere. To reduce the total amount of readout channels we have also tried to keep them as much as possible the same over a station.

The cell size of the outer tracker detectors is chosen such that all drift signals arrive at the preamplifiers within 50 ns after the bunch crossing [2]. This implies that track signals from at most two consecutive bunch crossings may overlap. Due to slower drift inside a magnetic field stations inside the magnet only contain chambers with cells of 5 mm diameter, while the stations in the field free region also contain cells of 8 mm diameter.

For the inner tracker the strip size depends on the chosen technology. Here we have chosen for an inner detector setup in which all sectors have equal pitch size. This means that only chambers of type I and II are used, which were granulated into 500 μm cells.

We assume that each measurement plane contains a number of wires or strips which perform a one dimensional measurement. A station then consists of a number of layers, where in each layer the measurement coordinate can be specified (x, y or a stereo angle u). The default setup is shown in table 2. A standard tracker station consists of 4 single (inner tracker) or double (outer tracker) layers, measuring respectively the x-coordinate, a -5^o stereo angle, a $+5^o$ stereo angle, and again an x-coordinate.

In addition the stations closest to the RICH1 and RICH2 detectors contain one (inner) or two (outer) extra layers with y-coordinate measurement.

The z-positions of the stations are chosen in a detailed optimization process. The criteria are: a good pattern recognition performance both in trigger and offline, an optimal track momentum reconstruction and precise position measurement. This optimalization is described in an LHCB note on track reconstruction. [4].

Station #	Layer Setup					
	1	2	3	4	5	6
1	x	-s	+s	x	y	y
2	y	y	x	-s	+s	x
3-9	x	-s	+s	x		
10	x	-s	+s	x	y	y
11	y	y	x	x		

Table 2: The default layer setup of each tracking station. Indicated are: `x`: x-coordinate measurement, `y`: y-coordinate measurement, `-s`: negatively tilted stereo measurement, `+s`: positively tilted stereo measurement. The stereo angles are set by default to -5^o and $+5^o$. For the outer tracker each detection layer actually consists of two staggered monolayers.

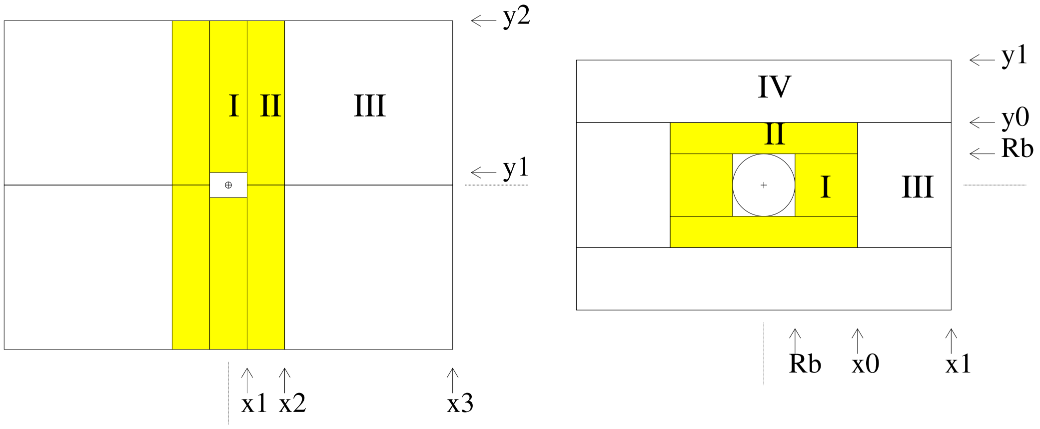

Figure 3: Logical segmentation for the a) Outer tracker b) Inner tracker
In both the inner and outer tracker, regions with relatively high and low granularity can be simulated.

4 Occupancies

The occupancies in each of the stations are calculated at the z-positions given in table 3.

We define the occupancy per wire (outer tracker) or per strip (inner tracker), as the fraction of pp interactions in which that particular wire was hit. In fig 4 we show examples of occupancy distributions for four inner and four outer tracker chambers. From these plots we observe that the hottest channels are always those closest to the beam pipe. Depending on the sector number, this is either at the left side or in the center of the plot.

A summary of all occupancies is plotted in fig 5. The "hottest area" plots represent the occupancy in the region of each sector where the occupancy is highest. The "average" plots give the average occupancy of a sector. In the chosen outer tracker setup the "hottest area" occupancy is less than 10% everywhere. The most densely populated areas are the upstream stations (before and inside the magnet) and the station downstream the RICH2. In general occupancies in the inner tracker are somewhat lower than those in the outer tracker.

The occupancy numbers presented here are valid for a bunch crossing with single pp interaction. Obviously, the occupancies depend on the number of pp interactions per bunch crossing and thus on the luminosity. For an average luminosity of $\mathcal{L} = 2\times10^{32}\mathrm{cm}^{-2}\mathrm{s}^{-1}$ the rate for single and multiple interactions are given in table 4 [5]. These numbers translate into the following situations: in 80.1% of the events the presented occupancies can be used directly, in 13.0% of the events they should be multiplied with a factor of 1.5, and in 6.9% of the events with a factor of 2.

station #	z position	x_0	x_1	x_2	x_3	y_0	y_1
1	100.	39.5	39.5	39.5	39.5	31.5	31.5
2	217.	30.0	30.0	94.5	94.5	20.0	75.5
3	330.	30.0	30.0	142.0	142.0	20.0	113.5
4	425.	30.0	30.0	191.0	191.0	20.0	146.0
5	565.	30.0	30.0	191.0	191.0	20.0	146.0
6	700.	30.0	30.0	90.0	217.0	20.0	179.0
7	890.	30.0	30.0	90.0	249.5	20.0	206.0
8	840.	30.0	30.0	90.0	265.0	20.0	219.0
9	890.	30.0	30.0	90.0	280.0	20.0	231.5
10	940.	30.0	30.0	90.0	296.0	20.0	244.5
11	1160.	30.0	30.0	90.0	359.0	20.0	296.5

Table 3: The sectioning of the stations. The following points should be noted: 1) Station 1 is purely built using inner tracker technology. 2) The inner tracker is not split in two "pitch areas", i.e. chambers of type III and IV are not used. 3) The outer tracker stations 2, 3, 4 and 5 only contain chambers of type II and III, i.e. only "small pitch" detectors.

$\mathcal{L} = 2 \times 10^{32}\mathrm{cm}^{-2}\mathrm{s}^{-1}$	$N_{int} = 1$	$N_{int} > 1$
No pile-up veto	9.39 MHz	3.01 MHz
Using pile-up veto	8.92 MHz	0.60 MHz

Table 4: Frequency of bunch crossing for one or more than one interaction, with and without use of the pile-up veto trigger. The numbers were calculated for the indicated average luminosity.

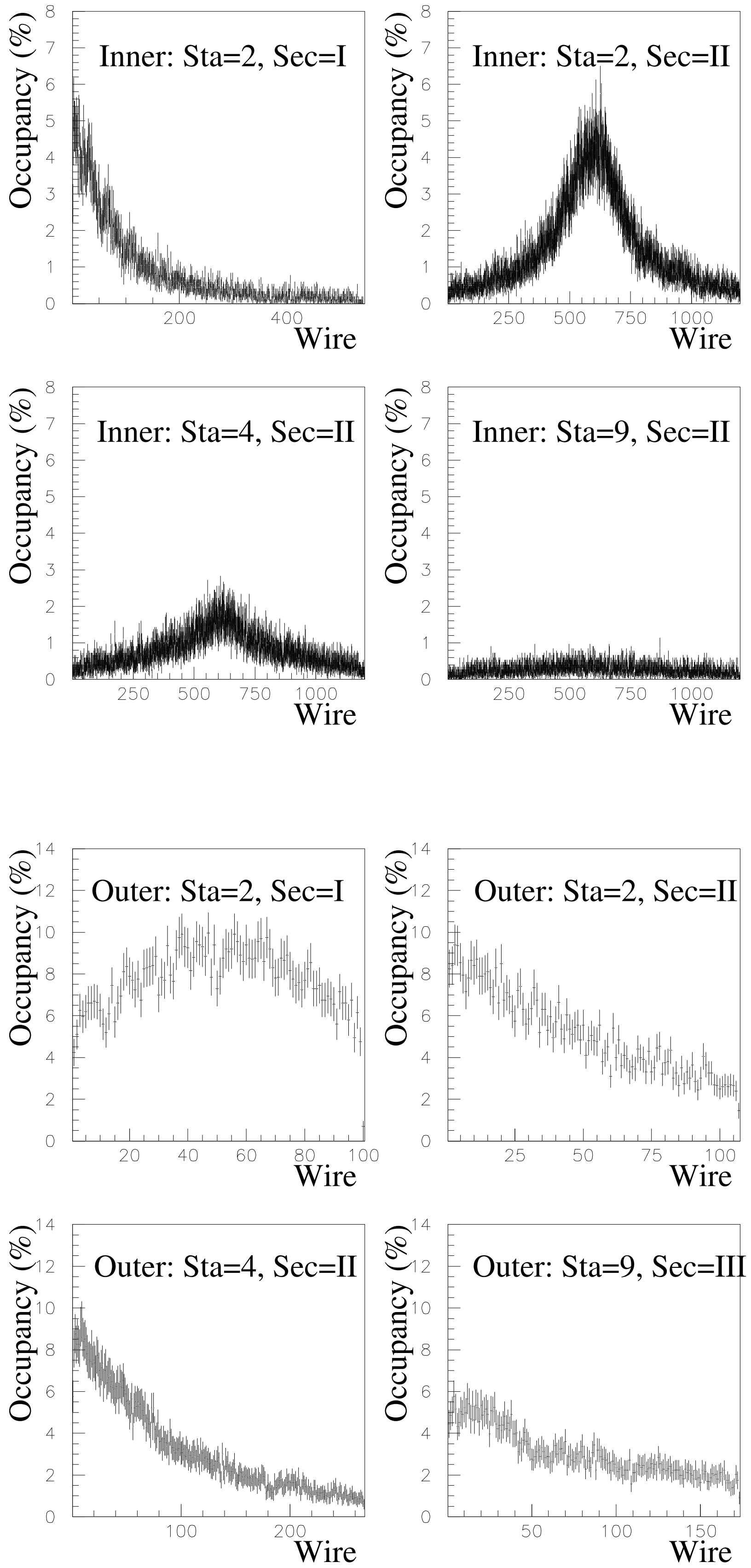

Figure 4: Examples of occupancy distributions vs wire number in a sector, for inner tracker (top 4 plots) and outer tracker (bottom 4 plots).

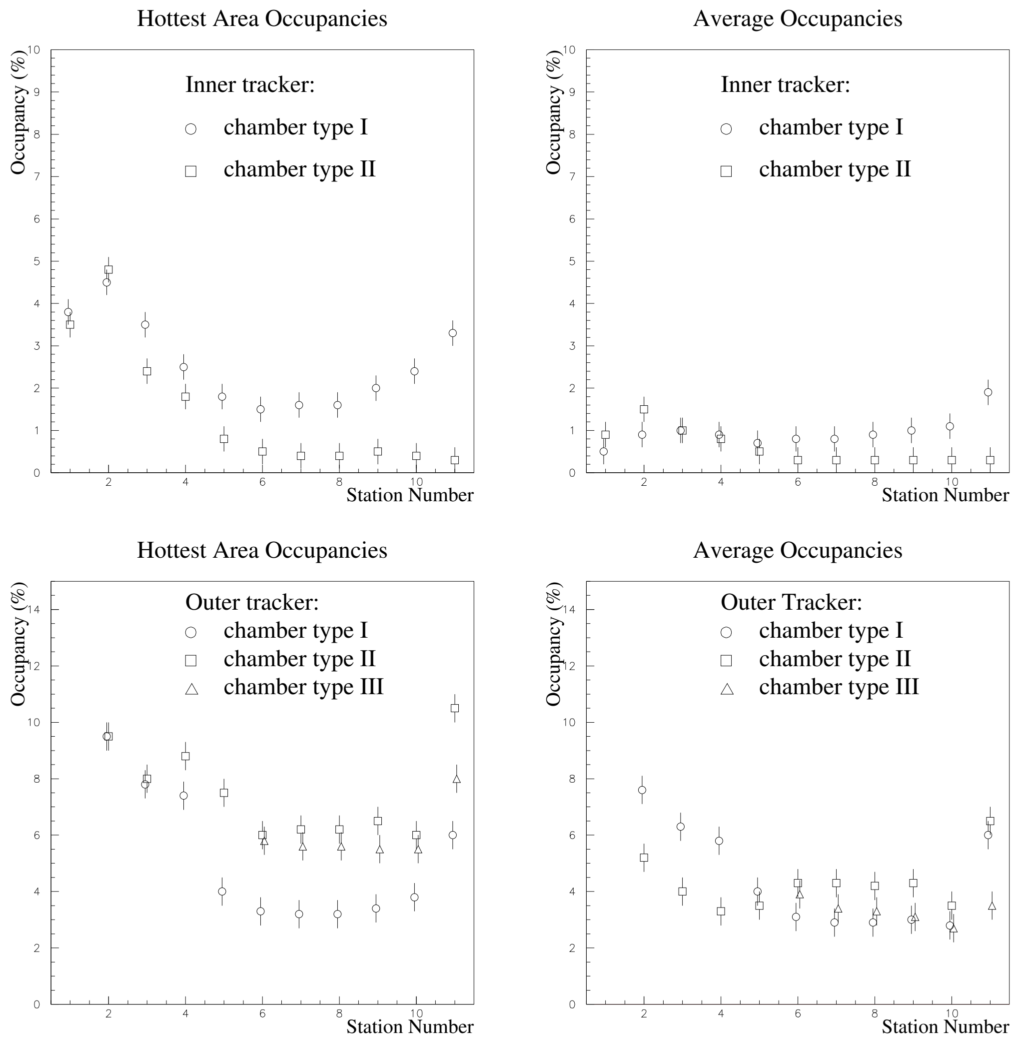

Figure 5: The *average* and *hot area* occupancies per station for inner and outer tracker.

References

[1] A. Tsaregorodtsev, "SICB user guide, GEANT3 based simulation package for the LHCB Experiment", june 19, 1997.

[2] Tracking chapter of the LHCB Technical Proposal.

[3] B. Koene et. al, technical note on LHCB Outer Tracker hardware for the Technical Proposal.

[4] R. v/d Eijk et. al, "Track Reconstruction for LHCB", LHCB internal note for the Technical Proposal.

[5] Trigger chapter of the LHCB Technical Proposal.